International Journal on Emerging Technologies **2**(2): 64-68(2011)

ISSN No. (Print) : 0975-8364
ISSN No. (Online) : 2249-3255

Perform Image Fusion Based Multi Resolution Curyelet and Framework System

Jincy John and Vibha Gupta

Department of Electronics and Communication RITS, Bhopal, (MP)

(Received 17 September, 2011, Accepted 5 October, 2011)

ABSTRACT : The image fusion is to integrate complementary information from several images to create a highly informative image which is more suitable for human visual perception or computer-processing tasks. Recent studies show that stationary wavelet transform (SWT) and non sub sampled contour let transform (NSCT) both turn out to be effective an deficient for image fusion. In order to take some complementary characteristics between the two muli resolution transformations simultaneously, we propose a hybrid multi resolution method by combining the SWT with the NSCT to perform image fusion. Two methods, serial NSCT aiding SWT (SNAS) and serial Standing NSCT (SSAN), are studied and compared with some state-of-the-art methods. Experimental results demonstrate that the SSAN method performs better than SNAS and the individual multi resolution-based methods, such as NSCT, SWT, complex wavelet (CWT), curve let (CVT) and wavelet-based contour let (WBCT).

Keywords: Terms-Image fusion, multisensor fusion, non sub sampled contour let transform (NSCT), stationary wavelet transform (SWT), hybrid muli resolution.

I. INTRODUCTION

Image fusion has become an important and useful technique for image analysis and computer vision. It is being studied and applied to integrate information from several images which may come from one sensor or multiple sensors. The fused image is more suitable for human perception or further image processing tasks [1], [2]. The fusion process can be performed at different levels of information representation, namely, pixel level, feature level and decision level [3]. Pixel level image fusion generates a fused image in which each pixel is determined by a set of pixels in various sources. The advantage of pixel level fusion is that the fused image contains more original information. In addition, compared to feature or decision level fusion, the pixel level fusion is easy to implement and more time efficient [4]. A simple image fusion method is to take the average of the source images pixel by pixel. Although this method is simple to implement, it brings about several undesired side effects including reduced contrast [4]. Multiscale transforms have been successfully used to image fusion in recent years. There is evidence that the human visual system performs similar signal decomposition in its early processing [5]. Commonly used multi resolution transformations include the Laplacian pyramid [6], ratio-of-low-pass pyramid [7], independent component analysis [8], and discrete wavelet transform (DWT) [9]-[13].The multiscale decomposition-based image fusion approaches have been studied within a generic image fusion framework in [4]. The basic idea is to perform certain multi resolution decomposition on each source image, and then integrate allthese decompositions to obtain one combined representation according to a fusion rule. Finally, applying the inverse transformation to the combined representation, the fused image can be constructed. The key step in multiscale decomposition- based image fusion is how to represent the details in the source images with decomposed coefficients. However, due to the down-sampling process, many multi resolution decompositions are not translation-invariant. Hence, in practice, their performances quickly deteriorate when there is a slight object movement or the source images cannot be perfectly registered. One way to alleviate this problem is to use translation-invariant multi resolution transformations, such as stationary wavelet transform (SWT) [14], [15]. The SWT closely resembles the DWT, but uses an over complete wavelet decomposition by avoiding DWT's down-sampling process. However, recent papers argued that wavelets and related classical multi resolution transforms are playing with a limited dictionary made up of roughly isotropic elements occurring at all scales and locations. To solve this problem, some new multiscale transformations like curve lets [16], ridge lets [17] and contourlets [18] are introduced. The main motivation of these new multiscale transformations is to pursue a "true" two-dimensional transform that can capture the intrinsic geometric structure. The ridgelet transform is applied to image fusion. The experimental results demonstrate that this algorithm outperforms classical fusion methods both in visual and objective evaluation. In curvelet transform is used to fuse remote sensing images. The experimental results show that the method simultaneously provides richer information in spatial and spectral domains. One contour let-based image fusion method is proposed, which is better in preserving edge and texture information than wavelet transform or Laplacian pyramid-based methods. Naturally, combining some complementary multiresolution methods to improve image fusion performance may be considered. In this paper, a hybrid multiresolution image fusion method using NSCT and SWT is proposed. Here, two proposed methods, the serial NSCT aiding SWT (SNAS) and the serial SWT aiding NSCT (SSAN), are investigated in this paper. The serial methods firstly decompose the source images into the high-frequency coefficients and the low-frequency coefficients using one transform. Then, the high-frequency coefficients are combined by selecting

coefficients with largest energy, and low frequency coefficients are combined using the other transform based image fusion method. The remaining sections of this paper are organized as follows. Section II briefly introduces the SWT, NSCT, and generic image fusion method based on multiresolution analysis. Section III provides the proposed fusion scheme. Section IV presents experimental results, and Section V summarizes this paper.

II. SWT, NSCT AND GENERIC IMAGE FUSION METHOD

The SWT [14], [15] is similar to the DWT, except that coefficient sequences are not decimated at each stage. It is a redundant scheme, as each set of coefficients contains the same number of samples as the input. The SWT provides the approximate shift invariance which the traditional wavelet transform is short of as the DWT, the SWT can well represent the small features, such as angles and textures. However, the SWT suffers from the drawbacks of limited directional information, and the lack of correlation of significant wavelet coefficients along the discontinuity curve. As a result, poor representations of edges are produced, particularly when images have contours and curves. The NSCT is a flexible multiscale, multidirectional, and shift-invariant image decomposition scheme which is built upon nonsubsampled multiscale pyramids and nonsubsampled of images very well, which is useful to many image processing directional filter banks . It can extract the geometric information tasks. Contour let represents the long edges very well while challenged by small features .

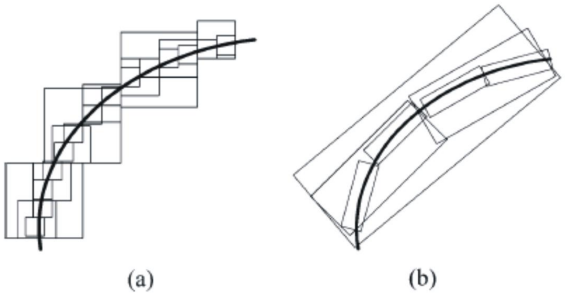

Fig. 1. Wavelet and contour let schemes in successive refinement near a smooth contour. (*a*) Wavelet. (*b*) Contour let.

Consider the situation when a smooth contour is being painted, as shown in Fig. 1. It illustrates the successive refinement by the two systems near a smooth contour. Since 2-D DWT is constructed from tensor products of 1-D DWT, the "wavelet"- style painter is limited to using square-shaped brush strokes along the contour, different sizes corresponding to the multiresolution structure of wavelets. As the resolution becomes finer, we can clearly see the limitation of the wavelet style painter who needs to use many fine "dots" to capture the contour. The contourlet, on the other hand, exploits effectively the smoothness of the contour by making brush strokes with different elongated shapes and in a variety of directions following the contour. However, the contourlet cannot represent small features such as angles as efficiently as the wavelet transform does. Considering an image "Lenna" with size 512 512, we do NSCT and SWT decomposition and reconstruction to compare their performances. For the NSCT, the contourlet transform is implemented into two levels, and each level contains eight orientations. For the SWT, the wavelet basis "Daubechies 6" and a decomposition level of 2 are used. The sum square of each high-frequency coefficient for each pixel location is calculated. We select all the low-frequency coefficients and those high-frequency coefficients with the top 2% largest sum squares to do reconstruction. The zoomed left eye regions of two reconstructed images by NSCT and SWT are shown in Fig. 2. A careful inspection reveals that the fringe of the hat in Fig. 2 (*b*) is smoother and clearer than it is in Fig. 2 (*a*), but in Fig. 2(*a*), Lenna's eye is clearer than it is in Fig. 2 (*b*). This example verifies that the NSCT and SWT have complementary characteristics. The multiresolution transforms, such as DWT, SWT, NSCT, complex wavelet transform (CWT), and curvelet (CVT) are appropriate for performing image fusion tasks. The generic image fusion schematic diagram is shown as Fig. 3. T represents the linear invertible transform while indicates the inverse transform. We assume that the source images have been registered. The fusion procedure takes the following steps. Firstly, Each of the registered input images $I_1 \ldots I_n$, is decomposed with certain multiresolution analysis method. The corresponding coefficients $C_1 \ldots C_n$, are obtained. Then, the coefficients are integrated according to certain fusion rule. Optionally, consistency verification is performed to ensure that a fused coefficient does not come from a different source image from most of its neighbors. Finally, the fused image is reconstructed by performing the corresponding inverse transform

LI and Yang: Hybrid Multiresolution Method for Multisensor Multimodal Image Fusion

Fig. 2. Comparison between the NSCT and SWT reconstructed results. (*a*) SWT-based method. (*b*) NSCT-based method.

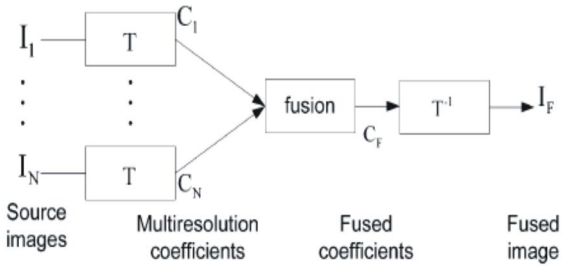

Fig. 3. Basic structure of generic image fusion method.

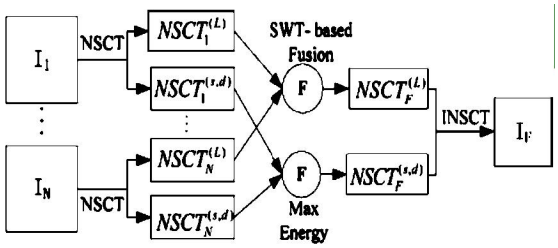

Fig. 4. Schematic diagram of SSAN.

III. THE HYBRID IMAGE FUSION METHOD

In this section, we design two different hybrid methods. These methods consider the SWT coefficients and NSCT coefficients simultaneously in the process of image fusion. We know that although different multiresolution analysis methods similarly decompose the input images into low-frequency and high frequency sub bands, the low-frequency coefficients or high-frequency coefficients among different decompositions have different characteristics. Thus, fusing the low-frequency and high-frequency coefficients using different suitable multiresolution methods can improve the performance of image fusion. Based on this idea, we design two multiresolution-based fusion methods: the serial SWT aiding *NSCT* (SSAN) and the serial *NSCT* aiding SWT (SNAS). Fig. 4 shows the schematic diagram of the serial method SSAN. The source images I_1, ….., I_n, are decomposed using the. NSCT, and the high-frequency coefficients. $NSCT^{(L)}$ are combined by selecting those with larger activity values, while the low-frequency coefficients $NSCT^{(s,\,d)}$ are fused using the SWT-based fusion method. The SSAN method is described in each of the source images, is decomposed by the *NSCT* into low-frequency coefficients and high-frequency coefficients, A^{NSCT}, 2. For every source image, the activity level of each *NSCT* coefficients, is calculated by the following two equations [4]:

$$E^{NSCT}(i,j) = \sum_{s=1}^{S}\sum_{d=1}^{D}[NSCT^{(s,d)}(i,j)]^2 \qquad \text{... (1)}$$

$$A^{NSCT} = W * E^{NSCT} \qquad \text{... (2)}$$

where D is the number of decomposition scales and S is the total number of frequency orientations, and

$$W = \frac{1}{256}\begin{bmatrix} 4 & 4 & 4 & 4 & 4 \\ 4 & 16 & 15 & 16 & 4 \\ 4 & 16 & 64 & 16 & 4 \\ 4 & 16 & 16 & 16 & 4 \\ 4 & 4 & 4 & 4 & 4 \end{bmatrix} \qquad \text{... (3)}$$

The convolution kernel W is applied to make the algorithm robust to variant adverse effects, such as misregistration and impulse noise, by collaboration from neighboring pixels. Here W, approximates a Gauss filter with cutoff frequency 0.3027. In fact, other possible filters with similar characteristics can also be used.

The high-frequency coefficients, $NSCT^{(s,\,d)}$, are combine by selecting the coefficients with larger energy as follows:

$$NSCT_F{}^{(s,d)}(i,j) = NSCT_m{}^{(s,d)}(i,j)$$
$$s = 1, \ldots..,\ S,\ d = 1, \ldots..,\ D \qquad \text{... (4)}$$

where $m = arg_n \max[A_n{}^{NSCT}(i,j)]$, the activity level. $A_n{}^{NSCT}$, of the high-frequency coefficients $NSCT^{(s,\,d)}$, is computed using (1) and (2).

The low-frequency coefficients, $NSCT^{(L)}$, are fused by using the generic multiresolution image fusion method described in Section II, where SWT is used. For SWT, the wavelet basis is "Daubechies 6," and the decomposition level is two. The activity level of each coefficient is calculated by weighted averaging over a 5 5 window at each coefficient location. The choosing maximum activity level technique is used to combine the SWT coefficients. The fused coefficients are indicated as $NSCT_F{}^{(L)}$.

The inverse *NSCT*(INSCT) is applied to the fused coefficients to get the fused image. The serial SNAS method is similar to the SSAN method. The source images are first decomposed by the *SWT*. The high-frequency coefficients, $SWT^{(s,\,d)}$, are fused by selecting the coefficients with larger energy at each pixel location, and the low-frequency coefficients, $SWT^{(L)}$, are fused by using the *NSCT* based fusion method, as described in Section III. Finally, the inverse *SWT* is applied to the fused coefficients to get the fused image.

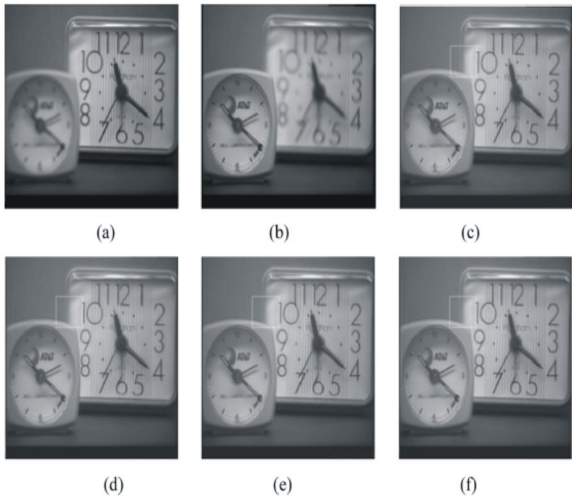

(*a*) focus on the right clock; (*b*) focus on the left clock; and (*c*)-(*f*) are the fusion

Fig. 5. Multifocus source images (256 level, 512 ? 512) and fusion results.

Zoomed image regions with size of 8080 From Fig. 5 (*c*)-(*f*): (*a*) From Fig. 5 (*c*); (*b*) From Fig. 5 (*d*); (*c*) from Fig. 5 (*e*); (*d*) from Fig. 5 (*f*).

IV. EXPERIMENTS

A. Experimental Setups

The experiment is done by a personal computer with 2.17 GHz CPU, 3GB RAM, under MATLAB 7.8. We use three scales of decomposition for NSCT, and two scales of

high-frequency coefficients are obtained. For the coarser scale, there are two directions, and for the finer, there are eight directions. Thus, for each source image, 11 subimages with the same size as the source image are generated. For SWT, the wavelet basis is "Daubechies 6," which behaves well in the preservation of original information, and the decomposition level is two, which results in seven subimages for each source image. In this work, we use both subjective and objective evaluations to test the fused results. The subjective method judges the quality of the image visually. Three objective image quality index, root mean squared error (RMSE), the metrics are also used. The RMSE between the ground truth fused image and the fused image is calculated to evaluate the image fusion performance. The lower the value of RMSE is, the better the fused image is [4]. The metric was proposed by Xydeas and Petrovic, which considers the amount of edge information transferred from the input images to the fused image. Sobel edge detector is used to calculate the strength and orientation information of the edge at each pixel in both source and the fused images. It should be close to 1 as much as possible.

B. Experimental Results

Fig. 5 (*a*) and (*b*) show a pair of tested images, each of which contains two clocks with different distances to the camera. The focus in Fig. 5 (*a*) is on the right clock, while the focusin Fig. 5 (*b*) is on the left one. Fig. 5 (*c*) and (*d*) illustrate the fused images using the *NSCT*-based and *SWT*-based image (*f*) are the fused results of the proposed SNAS and SSAN,respectively. It is difficult to conclude which resultant image is the best from visual observation since only a slight difference can be found among them. Therefore, for further comparison, we magnify one selected region, as shown in Fig. 6, from the resulted images in Fig. 5. Comparing Fig. 6 (*a*) and (*b*), we can see that the result of the *NSCT* method retains more edge information than the result of the *SWT* method. The results of the hybrid methods SNAS and SSAN shown in Fig. 6 (*c*) and (*d*) are both better than the results of the *SWT* or the *NSCT* methods. The edges in Fig. 6 (*c*) and (*d*) are clearer than those in Fig. 6 (*a*) and (b), and the angle point of the two edges with different orientation in Fig. 6 (*c*) and (*d*) is also clearer. Further, comparing Fig. 6 (*c*) and (*d*), we can see that Fig. 6 (*d*) is more acceptable which has fewer artifacts contained. This may be due to that the SSAN considers both the *NSCT* and the *SWT* simultaneously. Notice that the SNAS method also considers both the *NSCT* and the *SWT*, but the result is not as good as that of SSAN method. As mentioned above, the low-frequency coefficients or high-frequency coefficients among different decompositions have different characteristics, and the edge information which is very important for visual perception mainly contains in the high-frequency coefficients. As the *NSCT* represents the long edges very well, the SSAN by which the high-frequency information is fused by using the *NSCT* coefficients is more appropriate than the SNAS. In addition, the low-frequency coefficients are further decomposed and fused by the *SWT*. Thus, more underlying information is transferred into the fused image making it well improved. illustrates a magnetic resonance image (MRI) of the same person. The experimental setups are the same as previously mentioned. The fused images are we can observe (*g*) preserve more useful information compared with others, and the distinct extent of the fusion image is improved. Another experiment is performed on visible and infrared images visual image which clearly shows grass. a thermal infrared image in which the target (the gun) is clearly visible. A careful inspection of the fusion results contains more details. In addition, in order to make the comparison as fair as possible, some multifocus images obtained by camera shown in the total number of frequency orientations, and The convolution kernel is applied to make the algorithm robust to variant adverse effects, such as misregistration and impulse noise, by collaboration from neighboring pixels. Here, approximates a Gauss filter with cut off frequency 0.3027. In fact, other possible filters with similar characteristics can also be used 3. The high-frequency coefficients, are combined by selecting the coefficients with larger energy as follows: are used in following experiments. From each image in two out-of-focus images are created by Gaussian blurring. Then, the blurred images with different focus points are taken as the source images. The original image is taken as the reference image. The values of and of the different proposed image fusion methods on the images are where the values in bold indicate the highest accuracy obtained over all the methods tested. We can see from that the SSAN provides the fused image with the largest value. For the SSAN method performs better than other methods for the natural source images. However, for the artificial images in the values of various fusion methods are almost unchanged. This may be due to that is not as sensitive as for the artificial images. The values of RMSE of the fusion results on those artificial blurred images generated from that the SSAN has the best performance in all of the investigated methods. Both objective and subjective analysis of the experimental results show that the SSAN has the highest quality performance. In the following section, the SSAN method is further studied and compared with some state-of-the-art algorithms. Here, the (CVT) and wavelet-based contourlet transform (WBCT) are used for comparison. For the complex wavelet-based method, the decomposed scale is 2. The subband consistency and majority consistency are used. For the curvelet-based method, the decomposed level 2 is used [34]. The fusion method based on WBCT is also a hybrid multi resolution-based method in some degree, which considers both the wavelet and the directional contourlet transform. Since both wavelet and contourlet contain the down sampled process, WBCT is a shift-variant image decomposition scheme. For WBCT-based fusion, we used three wavelet levels and directional sub bands for three wavelet levels from the coarser to the finer. Three different scale and direction cases, , and are used to investigate the effects of various decomposition scales and directions of NSCT on the fusion performance of the SSAN method. The values of the fused results using different methods on all the source images are listed in lists the values of different methods on the Fig. 6.

(a) (b) (c) (d)

Fig. 6.

V. CONCLUSION

In this paper, we first briefly analyze the complementary characteristics between the stationary wavelet transform and the nonsubsampled contourlet transform by comparing the differences between the reconstructed images. Then, the serial hybrid fusion schemes are proposed for exploring the complementary characteristics between different multi resolution methods in fusion processes. Objective and subjective comparisons between the different combined fusion methods have been implemented. Experimental results on several multisensor images show that the SSAN method performs better than the SNAS and, in most cases, performs better than the individual multi resolution-based methods, including *NSCT*, *SWT*, CWT, CVT, and WBCT. Some parameters affecting the performance are also investigated. From the experimental results we can see that the increase of decomposed levels and directions can improve the fused result of the best serial method, SSAN. A shortcoming of the hybrid multi resolution method is that it.

REFERENCES

[1] J. K. Aggarwal, Multisensor Fusion for Computer Vision. Berlin,Germany: Spinger-Verlag, (1993).

[2] R.C. Luo, C.C. Yih, and K.L. Su, "Multisensor fusion and integration: Approaches, applications, and future research directions," *IEEE Sensors J.*, vol. **2**, no. 2, pp. 107-119, (2002).

[3] N. Cvejic, D. Bull, and N. Canagarajah, "Region-based multimodalimage fusion using ICA bases," *IEEE Sensors J.*, vol. **7**, no. 5, pp. 743-751, May (2007).

[4] Z. Zhang and R.S. Blum, "A categorization of multiscale-decomposition-based image fusion schemes with a performance study for a digitalcamera application," *Proc. IEEE*, vol. **87**, no. 8, pp. 1315-1326, (1999).

[5] D.L. Donoho and A.G. Flesia, "Can recent innovations in harmonicanalysis 'explain' key findings in natural image statistics," *Network:Computation in Neural Systems*, vol. **12**, no. 3, pp. 371-393, (2001).

[6] P.T. Burt and E.H. Andelson, "The Laplacian pyramid as a compactimage code," *IEEE Trans. Commun.*, vol. **31**, no. 4, pp. 532-540, (1983).

[7] A. Toet, "Image fusion by a ratio of low-pass pyramid," *Patt Recog. Lett.*, vol. **9**, no. 4, pp. 245-253, (1989).

[8] N. Mitianoudis and T. Stathaki, "Optimal contrast correction for ICA based fusion of multimodal images," *IEEE Sensors J.*, vol. **8**, no. 12, pp. 2016-2026, Dec. (2008).

[9] H. Li, B. Manjunath, and S. Mitra, "Multisensor image fusion using the wavelet transform," Graph. *Models Image Process.*, vol. **57**, no. 3,pp. 235-245, (1995).

[10] G. Pajares and J. Cruz, "A wavelet-based image fusion tutorial," *Patt. Recog.*, vol. **37**, no. 9, pp. 1855-1872, (2004).

[11] Y. Chibani and A. Houacine, "Redundant versus orthogonal wavelet decomposition for multisensor image fusion," *Patt. Recog.*, vol. **36**, no.4, pp. 1785-1794, (2003).

[12] P. Hill, N. Canagarajah, and D. Bull, "Image fusion using complexwavelets," in Proc. 13th Brit. Machine Vision Conf., Cardiff, U.K., (2002), pp. 487-496.

[13] S.T. Li, J.T. Kwok, I. W. Tsang, and Y.N. Wang, "Fusing images withdifferent focuses using support vector machines," *IEEE Trans. Neural Net.*, vol. **15**, no. 6, pp. 1555-1561, (2004).

[14] M. Beaulieu, S. Foucher, and L. Gagnon, "Multi-spectral image resolutionrefinement using stationary wavelet transform," in Proc. IEEE Int. Geosci. Remote Sensing Symp., *Vancouver, Canada*, (1989), vol. **6**, pp. 4032-4034.

[15] O. Rockinger, "Image sequence fusion using a shift invariant wavelettransform," in Proc. Int. Conf. Image Proc., Washington, DC, (1997), vol. **3**, pp. 288-291.

[16] E.J. Candes, L. Demanet, and D.L. Donoho, "Fast discrete curvelettransforms," *Multiscale Modeling and Simulation*, vol. **5**, no. 3, pp. 861-899, (2006).

[17] M.N. Do and M. Vetterli, "The finite ridgelet transform for image representation," *IEEE Trans. Image Proc.*, vol. **12**, no. 1, pp. 16-28, (2003).

[18] M.N. Do and M.Vetterli, "The contourlet transform: An efficient directional multiresolution image representation," *IEEE Trans. Image Proc.*, vol. **14**, no. 12, pp. 2091-2106, (2005).